A new species of *Eomellivora* from the latest Aragonian of Abocador de Can Mata (NE
Iberian Peninsula)

David M. Alba[1,*], Josep M. Robles[1], Alberto Valenciano[2], Juan Abella[1,3], Isaac Casanovas-
Vilar[1]

[1] Institut Català de Paleontologia Miquel Crusafont, Universitat Autònoma de Barcelona,
Edifici ICTA-ICP, c/ Columnes s/n, Campus de la UAB, 08193 Cerdanyola del Vallès,
Barcelona, Spain

[2] Departamento de Ciencias de la Tierra and Instituto Universitario de Investigación en
Ciencias Ambientales de Aragón (IUCA), Área de Paleontología, Universidad de Zaragoza, C/
Pedro Cerbuna 12, 50009 Zaragoza, Spain

[3] Instituto Nacional de Biodiversidad, Pje. Rumipamba N. 341 y Av. de los Shyris (Parque La
Carolina) Quito, Ecuador

*Corresponding author. *E-mail address:* david.alba@icp.cat

ORCIDs:

David M. Alba: 0000-0002-8886-5580

Josep M. Robles: 0000-0002-5410-3529

Alberto Valenciano: 0000-0003-1633-2248

Juan Abella: 0000-0002-3433-6093

Isaac Casanovas-Vilar: 0000-0001-7092-9622

ABSTRACT

Eomellivora is a large-bodied mellivorine mustelid genus widely distributed throughout Eurasia and North America during the late Miocene (MN9-MN13). Here, we report the oldest Eurasian material of *Eomellivora* based on a palate and two mandibular fragments from ACM/PTA-A2, a pre-Vallesian (11.21 Ma; latest MN7+8) locality of Abocador de Can Mata (Vallès-Penedès Basin, NE Iberian Peninsula) that slightly predates the first appearance datum of *Hippotherium* by ~30 kyr. The described material differs from *Hoplictis helbingi*—another large mustelid recorded within the same basin in the roughly coeval site of Castell de Barberà (~11.2, earliest MN9)—and more closely resembles *Eomellivora* spp. Despite closer resemblances in both size and dental shape with the Vallesian (MN9–MN10) species *Eomellivora piveteaui*, the ACM material differs from multiple features that may be considered plesiomorphic. A new species, *Eomellivora moralesi* sp. nov., is thus erected based on the described material. A cladistic analysis confirms that the new species occupies a basal-most position within the *Eomellivora* clade, in agreement with its older age and more plesiomorphic morphology.

Introduction

Eomellivora Zdansky, 1924 is a giant and hypercarnivorous mustelid genus recorded from the Miocene of Eurasia (Wolsan and Semenov, 1996; Valenciano et al. 2015, 2017) and North America (Baskin 1988). Wolsan and Semenov (1996) distinguished a single species of *Eomellivora* (the nominotypical one) with two distinct (Vallesian and Turolian) chronosubspecies. However, the recent description of additional material led Valenciano et al. (2015, 2017) to recognize as much as five species (see Table S1 for a list of localities). Older records of *Eomellivora* from the middle Miocene of Asia (e.g., Patnaik 2013) are either doubtful or correspond to species excluded from *Eomellivora* (Wolsan and Semenov 1996), whereas ?*Eomellivora tugenensis* Morales and Pickford, 2005 from Kenya (~12–11.5 Ma; Werdelin and Peigné 2010) most likely belongs to a different genus (Valenciano et al. 2017; Valenciano and Govender 2020), probably more closely related to the Mellivorini than to the Eomellivorini. *Eomellivora* sp. has also been reported from pre-Vallesian levels in Hammerschmiede 5 (Germany, ~11.62 Ma; Kirscher et al. 2016), but the material is unpublished. Here we report a new species of *Eomellivora* that further indicates that the genus was already present in Europe slightly before the Vallesian.

Age and geological background

The described material comes from the local stratigraphic sequence of Abocador de Can Mata (ACM; Alba et al. 2006, 2017) in els Hostalets de Pierola (Vallès-Penedès Basin, NE Iberian Peninsula; Figure 1a). Continuous paleontological surveillance during the construction of a dump since 2002 has yielded thousands of fossil vertebrate remains that can be accurately dated thanks to litho-, bio- and magnetostratigraphic correlation (Casanovas-Vilar et al. 2016a, 2016b; Alba et al. 2017). The published composite sequence

3

spans from 12.6 to 11.4 Ma (Alba et al. 2017), but additional fieldwork in 2019–2020 extended the sequence toward the Vallesian.

The described material comes from locality ACM/PTA-A2 (Préstec de Terres de l'Abocador, subsector A, locality 2; Figure 1(b–c); Figure S1), which is situated in meter 268 of the ACM composite sequence and magnetostratigraphically correlated to the second portion of C5r.2n (i.e., postdating the short normal subchron C5r.2r-1), with an interpolated age 11.21 Ma and located only 5 m below the bottom C5r.1n (D.M.A. and J.M.R., unpublished data; see Figure S2). The beginning of the Vallesian in the Vallès-Penedès Basin, defined by the entry of hipparionin horses, is correlated to the base of C5r.1n, with an interpolated age of 11.18 Ma (Garcés et al. 1996; Casanovas-Vilar et al. 2016a, 2016b; Alba et al. 2019). Therefore, ACM/PTA-A2 can be securely correlated to latest Aragonian (MN7+8; *Democricetodon crusafonti – Hippotherium* Interval subzone of the Vallès-Penedès Basin; Casanovas-Vilar et al. 2016b), minimally predating the Vallesian by ~30 kyr.

Material and methods

The described material is housed at the Institut Català de Paleontologia Miquel Crusafont (ICP), Sabadell, Spain. It includes three dentognathic specimens recovered during April 2019 that might belong to a single individual, although the lack of contact and close spatial association makes it impossible to confirm this. Measurements were taken with a digital caliper to the nearest 0.1 mm. Maximum mesiodistal length (L) and buccolingual width (W) were measured and compared with data taken from the literature (Petter 1963; Wolsan and Semenov 1996 and references therein; Morales and Pickford 2005; Koufos 2012; Valenciano et al., 2015, 2017; Lavrov and Gimranov 2018) using bivariate plots. A robusticity index (in %) was also computed as RI=W/L × 100.

A cladistic analysis of *Eomellivora* spp. was performed based on a restricted subsample of the character-taxon matrix of Valenciano and Govender (2020; see character definition in Text S1), including three *Eomellivora* species, the mellivorin *Howellictis valentini* de Bonis et al., 2009, and the oligobunine *Zodiolestes daimonelixensis* Riggs, 1942 as outgroup. Two additional species of *Eomellivora* (based on Valenciano et al. 2017 and the Can Llobateres material described by Crusafont-Pairó 1972) and the new species described herein were also included in the analysis. The eomellivorin *Ekorus ekakeran* Werdelin, 2003 was excluded from the present analysis pending more detailed studies focused on the whole tribe. In turn, as in Valenciano and Govender (2020), the poorly known African eomellivorine ?*E. tugenensis* was excluded from the analysis because too few characters (15 out of 100) could be coded. Finally, the material from Gritsev assigned to *Eomellivora wimani* by Wolsan and Semenov (1996) and included in the morphometric comparisons as *Eomellivora* sp. was also excluded from the phylogenetic analysis pending its detailed description. The resulting matrix (Table 1) was analyzed using maximum parsimony with PAUP* v. 4.0a168 for Mac (Swofford 2003) with the 'branch and bound' option. All characters were treated as unordered and clade stability was assessed by means of bootstrap analysis (10,000 replicates) and Bremer indices.

Systematic paleontology

Order Carnivora Bowdich, 1821

Suborder Caniformia Kretzoi, 1943

Family Mustelidae Fischer, 1817

Subfamily Mellivorinae Gray, 1865

Tribe Eomellivorini Zdansky, 1924

Genus *Eomellivora* Zdansky, 1924

Emended diagnosis

Modified after Valenciano et al. (2017). Mellivorine mustelid of large size; P1 present; P3 with the distal area thickened (only incipiently in the most plesiomorphic species); P4 with a subconical protocone, and with paracone-protocone and paracone-parastyle crests; P4 protocone located in line with the parastyle; P4 parastyle poorly-developed but thickened; buccal wall of P4 with a concavity in the base of the crown between the paracone and the metastyle, exhibiting a variable degree of development; stylar area of M1 enlarged; M1 with a non-reduced metacone in the more plesiomorphic species and a reduced one in the more derived ones; M1 with an arched ridge-shaped or conical protocone continuing into the mesial protocone crest, and a talon relatively equally expanded mesially and distally; premolar teeth crowned; p1 present; p2 turned buccolingually from the tooth row; p3 with a distal accessory cuspid and with the distal area thickened; p4 enlarged with a distal accessory cuspid and with a backward inclination of the main cuspid towards the m1; m1 enlarged with a distinct metaconid in the most plesiomorphic species and vestigial to absent in the remaining ones, in which it is replaced by a distinct crest; m1 talonid with single but strong, high and centrally positioned hypoconid; m2 elongated mesiodistally with a low crown surrounded by a cingulum and a central protoconid.

Included species

Eomellivora wimani Zdansky, 1924 (type species); *Eomellivora fricki* (Pia, 1939); *Eomellivora hungarica* Kretzoi, 1942; *Eomellivora ursogulo* (Orlov, 1948); *Eomellivora piveteaui* Ozansoy, 1965; *Eomellivora moralesi* sp. nov.

Eomellivora moralesi sp. nov.

Holotype

IPS122262, palate with incisor, canine and left P1 alveoli, as well as left P2–M1 and right P1–M1 crowns (Figure 2(a–e, l–s)).

Paratypes

IPS122212, right mandibular fragment preserving the symphysis, c1–p1 alveoli, the complete p2 crown, and partial p3 (very damaged) and p4 (only mesial) crowns (Figure 2(f–h)); IPS122214, right mandibular fragment with m2 (Figure 2(i–j)).

Type locality

ACM/PTA-A2 (els Hostalets de Pierola, Catalonia, Spain).

Age and distribution

Only known from the type locality (11.21 Ma, latest Aragonian, MN7+8).

Etymology

Species trivial name dedicated to Prof. Jorge Morales, in recognition to his extraordinary contribution to vertebrate paleontology.

Diagnosis

Eomellivora species of moderate size (similar to *E. piveteaui*). P2 without distal accessory cusp and with a subrectangular occlusal profile that lacks a labial concavity. P3 slender, with a straight labial wall, a poorly developed basal cingulum, and without mesial and distal accessory cusps. P4 without a marked concavity on the labial wall or a marked basal cingulum. M1 slender, with a well-developed parastylar area and lingual platform (longer than the labial wall) that lacks a concavity at mid-length, a non-reduced metacone as well as a mesiolingually located protocone that bears a ridge-like extension and is not completely enclosed by the lingual platform. p2 moderately robust and without distal accessory cuspid. p3 moderately expanded distally. m2 with metaconid.

The new species differs from other *Eomellivora* spp. in the slenderer P3 without a distal accessory cusp, a marked labial concavity or a strong basal cingulum (tooth locus unknown in *E. fricki* and *E. hungarica*); the weaker P4 basal cingulum (tooth locus unknown in *E. hungarica*); and the retention of m2 metaconid (unknown in *E. fricki* and *E. hungarica*). It further differs from *E. piveteaui* in the larger parastylar area of the M1, and the subquadrangular lingual platform of the M1, and from *E. fricki* in the smaller size, the lower P4 protocone, and the less robust M1 with a less developed lingual platform. The new species more clearly differs from *E. wimani, E. ursogulo*, and *E. hungarica* in the more mesially located protocone and the non-reduced metacone (relative to the paracone) in the M1, and the lack of p4 mesial accessory cuspid. It further differs from *E. wimani* and *E. ursogulo* in other features unknown for *E. hungarica*: the subrectangular (instead of triangular) occlusal profile of the P2 with a straight (non-concave) labial wall, the lack of P3 mesial accessory cusp, the lack of a marked labial concavity on the P4, and the less robust p2; additionally from *E. wimani*, in the more ridge-like M1 protocone; and additionally from *E. ursogulo*, in the lack of distal accessory cusp in the P2, of a mid-length concavity on the

M1 lingual platform, and of a distal accessory cuspid in the p2, as well as in the less distally expanded p3.

Description

Craniodental measurements for the holotype and paratypes are reported in Tables 2–3 (see also Figure 3 for bivariate plots of tooth dimensions). The cranial fragment IPS122262 (Figure 2(a–e)) preserves the palate and the anteriormost portion of the zygomatic arches, which are crushed and held together by matrix. The specimen displays an overall massive aspect and preserves relatively well the original shape of the dental arcade. The infraorbital foramen is large (Table 3) and located at the level of the upper carnassial parastyle. The external border of the right C1 is broken away and both the right premaxilla and palatine process of the maxilla at the I3–P2 level are somewhat displaced from their anatomical position, but it can be ascertained that the right foramen incisivum would have been located at the mesial level of the C1 alveolus. No incisors are preserved, but the I1–I2 alveoli are transversely aligned and overlap with the anteriormost portion of the I3 alveolus. Based on alveolus size, the I3 crown would have been caniniform and much larger than the other incisors, but about half the size of the C1, which appears quite massive and only slightly labiolingually compressed in basal dimensions (estimated RI = 94%). There is a small diastema between the I3 and the C1.

Between the distolingual corner of the C1 alveolus and the P2 there is a unicuspid, uniradiculate and tiny P1, whose crown is only preserved on the right side. The P2 crown (Figure 2(l–m)) is biradiculate and displays a very slender (RI=61–62%), elliptical to subrectangular occlusal outline (much wider than long), with a straight labial and convex lingual sides. The P2 is rotated labially, its main cusp is mesially located, and it lacks a

9

distinct distal accessory cusp. The P3 (Figure 3(n–o)) is much larger than the P2. It is biradiculate and displays a subrectangular but slenderer contour (RI=55–56%) than the P2. The P3 lingual margin is bulging, whereas the labial wall is straight. This tooth has marked mesial and distal cingula, which nevertheless do not continue along the lingual or labial walls. There are no distinct mesial or distal accessory cusps, and indeed the thick and blunt crista that extends distalward from the main cusp apex fades away before reaching the distal margin.

The P4 (Figure 2(p–q)) is longer than the P3 (P4 L / P3 L = 147–149%) and also somewhat stouter than the preceding premolars (RI = 65–66%). The occlusal morphology is best preserved in the right P4, while the left one is distally damaged. There is some dentine exposure at the apices of the protocone and the paracone, as well as along the metastyle, which extends along about two-thirds of crown length. The crown displays a subtriangular occlusal profile with almost parallel (non-distally tapering) labial and lingual walls. The protocone is low and peripherally located on the protruding mesiolingual corner of the crown, being surrounded by a distinct cingulum. The parastyle is low and transversely aligned with the protocone. The crown displays a very slight mesial concavity between parastyle and protocone, and an almost straight buccal crown wall (with no distinct concavity distally from the paracone). The paracone is the highest and most extensive cusp; together with the metastyle it constitutes a moderately elongate, slightly labially concave blade. A distinct mesiolabial crista extends from close to the paracone apex to the parastyle, whereas a fainter mesiolingual crista links the paracone with the protocone. There is no well-developed cingulum surrounding the whole crown.

The M1 (Figure 2(r–s)) has a vaguely figure-eight shape, being considerably broader than long (RI=173–174%) but slightly narrower than the length of the upper carnassial (M1 W /

10

P4 L = 89–90%). The crown is markedly constricted at about mid-width, with an expanded lingual platform that displays a suboval (convex) profile and is much longer than the buccal half of the crown. The tooth is surrounded by a marked cingulum, well developed on the lingual side and on the labial side, where it constitutes a distinctly protruding (almost cuspule-like) stylar area. The paracone is bulbous and more extensive than the metacone, which is partially worn. The protocone is pyramidal but displays a ridge-like mesiolabial extension. It is centrally located on the labial moiety of the crown and is not completely enclosed within the lingual platform. There is no conspicuous crest linking the paracone with the protocone.

Based on IPS122212 (Figure 2(f–h)) and IPS122214 (Figure 2(i–k)), the morphology of the mandible can be only partially ascertained. The former specimen preserves most of the symphyseal suture (from the mesialmost level of the c1 alveolus) and the corpus up to mid-p4 level, whereas the latter preserves the posteriormost portion of the corpus (including the distal portion of the m1 alveolus) and the anteriormost portion of the ramus. The symphysis displays a gently convex anterior profile and inferiorly extends up to the p3 level, where the corpus is somewhat deeper than below the p4. Overall, the corpus appears dorsoventrally deep and labiolingually thick, being stouter at the c1 level than posteriorly (Table 3). There are two mental foramina slightly above corpus mid-height, one below the p2 and the other at the distal p3 level. There is a deep masseteric fossa that reaches its maximum depth at the distal m2 level but extends rostrally beyond the m2.

Based on alveolus size, the c1 would have been quite massive, displaying a slightly labiolingually compressed subelliptical basal contour (estimated RI=77%). There is a tiny p1 alveolus between the mesiolingual aspect of the p2 and the distal aspect of the c1 alveolus. The p2 (Figure 2(t)) is biradiculate and much longer than wide (RI=58%), with its main axis

labially rotated. There is no distinct distal accessory cuspid and there are no cingula other than the thickened distal crown margin. Based on its alveolus, the p3 would have been somewhat rotated labially, considerably longer than the p2 (12.4 vs. 8.7 mm, respectively), and slightly slenderer (estimated RI=52%), being wider distally than mesially. Although only the distalmost portion of the p3 is preserved, a distal accessory cuspid seems to have been present on the distolabial aspect of the main cuspid. Only the mesial portions of the p4 crown (including the apex of the main cuspid) and alveolus are preserved, making it impossible to ascertain the size and proportions of this tooth. There is no mesial accessory cuspid and the preserved portion of the labial wall appears straight. The size and proportions of the m1 cannot be adequately ascertained either. The m2 (Figure 2(u)) is obliquely inserted (relative to the occlusal plane of the remaining postcanine teeth). It displays a trapezoidal occlusal contour, being slightly longer than broad (RI=84%), particularly on the labial side, and possessing a markedly oblique distal margin. The protoconid is rounded and centrally located, but the mesial aspect of the m2 is worn away, making it impossible to ascertain the development of the paraconid. In contrast, a low but extensive and distally protruding hypoconulid is present on the distolabial corner of the crown. A distinct (albeit smaller) metaconid is also present on the lingual aspect of the protocone base.

Phylogenetic results

The phylogenetic analysis based on 24 parsimony-informative characters yielded 3 most parsimonious cladograms of 34 steps (Figure 4). The analysis fails to resolve the trichotomy between *E. wimani, E. ursogulo*, and *E. hungarica* but recovers *E. moralesi* sp. nov. as the

most basal species of the genus, followed by the successive branching of *E. fricki* and *E. piveteaui*.

Discussion and conclusions

Eomellivora moralesi sp. nov. from ACM generally fits Valenciano et al.'s (2017) emended diagnosis of *Eomellivora* (see also Figure 5), except for the presence of one or two distal accessory cusps in the P3. The ACM material further differs from other *Eomellivora* species in the retention of a metaconid in the m2. Accordingly, an emended diagnosis of the genus (modified after Valenciano et al. 2017) has been provided. Both features are probably plesiomorphic, in agreement with the somewhat older age of the new species and its greater similarities with the Vallesian species of *Eomellivora* (e.g., subrectangular P2 crown without a labial concavity; P3 without mesial accessory cusp; lack of a marked concavity on the labial wall of the P4; non-reduced M1 metacone; moderately robust p2; lack of p4 mesial accessory cuspid).

The retention of plesiomorphic features in *E. moralesi* sp. nov. agrees with our cladistic results indicating a basalmost position within the genus. ?*Eomellivora tugenensis* from Kenya (Morales and Pickford 2005), potentially ancestral to later *Eomellivora* (Valenciano et al. 2015, 2017), was excluded from the analysis because of excessive missing data. The small size, relatively large orbit size and lack of P1 suggest that ?*E. tugenensis* might be more closely related to mellivorins than to eomellivorins. In any case, the ACM material clearly differs from it by the larger size, the relatively smaller orbit, the more transversely aligned incisors, the less labiolingually compressed C1, the presence of a small diastema between the I3 and the C1, the presence of P1, the rotated orientation of the P2, the more robust P4, and the more distinct labial stylar area in the M1.

An alternative assignment of the ACM material to *Hoplictis* Ginsburg, 1961 can also be discounted based on the larger size of the former, the stouter P4 with a better developed protocone, and the non-reduced metacone and larger lingual platform of the M1 (Valenciano et al. 2019). Only *Hoplictis helbingi* (Viret, 1951), known by an m1 (lectotype; Depéret 1892: Pl. I fig. 3; Viret, 1951: Pl. II fig. 12a-b) and a P4 (paralectotype; Viret 1951: Pl. II fig. 13a–b) from La Grive-Saint-Alban (MN7+8), France, approaches the size of the ACM material. The lectotype of *H. helbingi* is virtually identical to that of a mandibular fragment (IPS33185) from Castell de Barberà (~11.2 Ma; Alba et al. 2019) assigned to the same species (Crusafont-Pairó 1972: Pl. 1 fig. 1; Valenciano et al. 2019: fig. 4l–n). Compared to the latter, the ACM material displays a deeper and stouter mandibular corpus, with the m2 alveolus being socketed obliquely (as it is typical of *Eomellivora*) instead of being on the same alveolar plane as the m1. The P4 from ACM further differs from the paralectotype of *H. helbingi* by being slightly larger and more robust, displaying parallel (instead of distally tapering) labial and lingual margins, and possessing a relatively larger and more mesially protruding protocone.

Eomellivora had not been reported as such from the Vallès-Penedès Basin until Valenciano et al. (2019) synonymized *Hoplictis petteri* (Crusafont-Pairó, 1972) with *E. fricki* based on the P4 holotype of the former (Fig. 5k) from Can Llobateres 1 (9.76 Ma; Casanovas-Vilar et al. 2016b), originally described by Petter (1963). The scarce material from Los Valles de Fuentidueña (MN9; Crusafont-Pairó and Ginsburg 1973; Ginsburg et al. 1981), previously assigned to *E. piveteaui* (Wolsan and Semenov 1996; Valenciano et al. 2015, 2017), might also be referrable to *E. fricki* based on the great development of the lingual platform and the distal expansion of the metacone in the M1 (Fig. 5r). Coupled with the material from Austria (Pia 1939; Zapfe 1948; Valenciano et al. 2017), this suggests that *E.*

fricki was widely distributed across Europe during the early Vallesian. However, an assignment of the ACM material to *E. fricki* can be ruled out based on its smaller size (Fig. 3) and other occlusal differences (Fig. 5). The ACM material is indeed more similar in size and occlusal morphology to *E. piveteaui* (Figs. 3 and 5), which is also known from the Spanish Vallesian (Batallones-3 and 10, MN10; Valenciano et al., 2015). Nevertheless, the ACM material from ACM differs from both *E. piveteaui* and *E. fricki* in multiple occlusal features present also in other *Eomellivora* (Figure 5), indicating that it belongs to a new, more plesiomorphic species. The somewhat older age of the new species further indicates that *Eomellivora* dispersed into (or locally evolved in) Europe sometime before the dispersal of hipparionin horses.

References

Alba DM, Moyà-Solà S, Casanovas-Vilar I, Galindo J, Robles JM, Rotgers C, Furió M, Angelone C, Köhler M, Garcés M, et al. 2006. Los vertebrados fósiles del Abocador de Can Mata (els Hostalets de Pierola, l'Anoia, Cataluña), una sucesión de localidades del Aragoniense superior (MN6 y MN7+8) de la cuenca del Vallès-Penedès. Campañas 2002-2003, 2004 y 2005. Estud Geol. 62:295–312.

Alba DM, Casanovas-Vilar I, Garcés M, Robles JM. 2017. Ten years in the dump: An updated review of the Miocene primate-bearing localities from Abocador de Can Mata (NE Iberian Peninsula). J Hum Evol. 102:12–20.

Alba DM, Garcés M, Casanovas-Vilar I, Robles JM, Pina M, Moyà-Solà S, Almécija S. 2019. Bio- and magnetostratigraphic correlation of the Miocene primate-bearing site of Castell de Barberà to the earliest Vallesian. J Hum Evol. 132:32–46.

Baskin JA. 1998. Mustelidae. In: Janis CM, Scott KM, Jacobs LL, editors. Evolution of Tertiary mammals of North America. Volume 1: Terrestrial carnivores, ungulates, and ungulatelike mammals. Cambridge: Cambridge University Press; p. 152–173.

Bowdich TE. 1821. An analysis of the natural classifications of Mammalia, for the use of students and travellers. Paris: J. Smith.

Casanovas-Vilar, I., Madern A., Alba DM, Cabrera L, García-Paredes I, Van den Hoek Ostende LW, DeMiguel D, Robles JM, Furió M, Van Dam J, et al. 2016a. The Miocene mammal record of the Vallès-Penedès Basin (Catalonia). C R Palevol. 15:791–812.

Casanovas-Vilar I, Garcés M, Van Dam J, García-Paredes I, Robles JM, Alba DM. 2016b. An updated biostratigraphy for the late Aragonian and the Vallesian of the Vallès-Penedès Basin (Catalonia). Geol Acta. 14:195–217.

Crusafont-Pairó, M. 1972. Les *Ischyrictis* de la transition Vindobonien-Vallésien. Palaeovertebrata. 5:253–260.

Crusafont-Pairó M, Ginsburg L. 1973. Les carnassiers fossiles de Los Vallès de Fuentiduena (Ségovie, Espagne). Bull Mus Natl Hist Nat. 131:29–45.

de Bonis L, Peigné S, Guy F, Likius A, Makaye HT, Vignaud P, Brunet M. 2009. A new mellivorine (Carnivora, Mustelidae) from the Late Miocene of Toros Menalla, Chad. N Jb Geol Paläontol. 252:33–54.

Depéret C. 1892. La faune de Mammifères Miocènes de La Grive-Saint-Alban (Isère) et de quelques autres localités du bassin du Rhone. Arch Mus Hist Nat Lyon. 5:1–95.

Fischer G. 1817. Adversaria zoologica. Mem Soc Imp Natural Moscou. 5:357–472.

Garcés M, Agustí J, Cabrera L, Parés JM. 1996. Magnetostratigraphy of the Vallesian (late Miocene) in the Vallès-Penedès Basin (northeast Spain). Earth Planet Sci Lett. 142:381–396.

Ginsburg L. 1961. La faune des Carnivores Miocènes de Sansan (Gers). Mém Mus Natl Hist Nat. 9:1–190.

Ginsburg L, Morales J, Soria D. 1981. Nuevos datos sobre los carnívoros de los Valles de Fuentidueña (Segovia). Estud Geol. 37:383–415.

Gray JE. 1865. Revision of the genera and species of Mustelidae contained in the British Museum. Proc Zool Soc Lond. 1865:100–154.

Kirscher U, Prieto J, Bachtadse V, Aziz HA, Doppler G, Hagmaier M, Böhme M. 2016. A biochronologic tie-point for the base of the Tortonian stage in European terrestrial settings: Magnetostratigraphy of the topmost Upper Freshwater Molasse sediments of the North Alpine Foreland Basin in Bavaria (Germany). Newslett. Stratigr. 49:445–467.

Koufos GD. 2012. New material of Carnivora (Mammalia) from the Late Miocene of Axios Valley, Macedonia, Greece. C R Palevol. 11:49–64.

Kretzoi M. 1942. *Eomellivora* von Polgárdi und Csákvár. Föld Közl. 72:318–323.

Kretzoi M. 1943. *Kochictis centennii* n. g. n. sp., ein altertümlicher Creodonte aus dem Oberoligozän Siebenbürgens. Föld Közl. 73:190–195.

Lavrov AV, Gimranov DO. 2018. First finding of a representative of giant mustelids of the genus *Eomellivora* (Carnivora, Mustelidae) in Russia (Tuva, Upper Miocene). Doklady Biol Sci. 480:82–84.

Morales J, Pickford M. 2005. Carnivores from the Middle Miocene Ngorora Formation (13-12 Ma), Kenya. Estud Geol. 61:271–284.

Orlov YU. 1948. *Perunium ursogulo* Orlov, a new gigantic extinct mustelid (a contribution to the morphology of the skull and brain and to the phylogeny of Mustelidae). Acta Zool. 29:63–105.

Ozansoy F. 1965. Étude des gisements continentaux et des mammifères du Cénozoïque de Turquie. Mém Soc Géol Fr. 44:1–92.

Patnaik, R. 2013. Indian Neogene Siwalik mammalian biostratigraphy. An overview. In: Wang X, Flynn LJ, Fortelius M, editors. Fossil mammals of Asia: Neogene biostratigraphy and chronology. New York: Columbia University Press; p. 423–444.

Petter G. 1963. Contribution a l'étude des Mustélidés des bassins néogènes du Vallès-Pénédès et de Calatayud-Teruel. Mem Soc Géol Fr. 97:5–44.

Pia J. 1939. Ein riesiger Honingsdachs (Mellivorine) aus dem Unterpliozän von Wien. Ann Naturhist Mus Wien. 50:537–583.

Riggs ES. 1942. Preliminary description of two Lower Miocene carnivores. Field Mus Nat Hist Geol Ser. 8:59–62.

Swofford DL. 2003. PAUP*. Phylogenetic Analysis Using Parsimony (*and other methods). Version 4. Sunderland: Sinauer Associates.

Valenciano A, Abella J, Sanisidro O, Harstone-Rose A, Álvarez-Sierra MÁ, Morales J. 2015. Complete description of the skull and mandible of the giant mustelid *Eomellivora piveteaui* Ozansoy, 1965 (Mammalia, Carnivora, Mustelidae) from Batallones (MN10), Late Miocene (Madrid, Spain). J Vertebr Paleontol. 35:e934570.

Valenciano A, Abella J, Göhlich UB, Ángeles Álvarez-Sierra M, Morales J. 2017. Re-evaluation of the very large *Eomellivora fricki* (Pia, 1939) (Carnivora, Mustelidae, Mellivorinae) from the late miocene of Austria. Palaeontol Electron. 20:17A.

Valenciano A, Jiangzuo Q, Wang S, Li C, Zhang X, Ye J. 2019. First record of *Hoplictis* (Carnivora, Mustelidae) in East Asia from the Miocene of the Ulungur River Area, Xianjiang, Northwest China. Acta Geol Sin. 93:251–264.

Valenciano A, Govender R. 2020. New fossils of *Mellivora benfieldi* (Mammalia, Carnivora,

Mustelidae) from Langebaanweg, 'E' Quarry (South Africa, Early Pliocene): Re-evaluation

of the African Neogene mellivorines. J Vertebr Paleontol. 40:e1817754.

Viret J. 1951. Catalogue critique de la faune des Mammifères Miocènes de la Grive Saint-

Alban (Isère). Première Partie. Chiroptères, Carnivores, Édentés Pholidotes. Nouv Arch

Mus Hist Nat Lyon. 3:1–102.

Werdelin L. 2003. Mio-Pliocene Carnivora from Lothagam, Kenya. In: Leakey MG, Harris JM,

editors. Lothagam: The dawn of humanity in Eastern Africa. New York: Columbia

University Press; p. 261–328.

Werdelin L, Peigné S. 2010. Carnivora. In: Werdelin L, Sanders WJ, editors. Cenozoic

mammals of Africa. Berkeley: University of California Press; p. 603–657.

Woslan M, Semenov YA. 1996. A revision of the late Miocene mustelid carnivoran

Eomellivora. Acta Zool Cracov. 39:593–604.

Zapfe H. 1948. Neue Funde von Raubtieren aus dem Unterpliozän des Wiener Beckens. Sitz-

Ber Öst Akad Wiss math-naturwiss Kl. 157:243–262.

Zdansky O. 1924. Jungtertiäre carnivoren Chinas. Palaeontol Sin C. 2:1–149.

Figure captions

Figure 1. a, Simplified geological map of the Vallès-Penedès Basin (modified from

Casanovas-Vilar et al. 2016a: fig. 1); the location of Abocador de Can Mata is denoted by a

black dot, whereas the top left inset denotes the location of the Vallès-Penedès Basin within

the Iberian Peninsula. b–c, Aerial photographs showing the location of locality ACM/PTA-A2

(geographic coordinates ETRS89: 1.799865E, 41.528243N) within the area affected by the

landfill construction (in 2017 and 2020) and in relation to farmhouses and the locality

ACM/BCV1 (b), as well as relative to subsector ACM/PTA-A and the farmhouse of Can Mata

de la Garriga (c). Base orthophotos were taken in 2019 (b) and 2021 (c); © Institut

Cartogràfic i Geològic de Catalunya, downloaded from VISSIR v. 3.26 and reproduced with

permission by means of a Creative Commons license CC BY 4.0 (ICGC, 2021). Abbreviations:

ACM = Abocador de Can Mata; BCV = Barranc de Can Vila; PTA = Préstec de Terres de
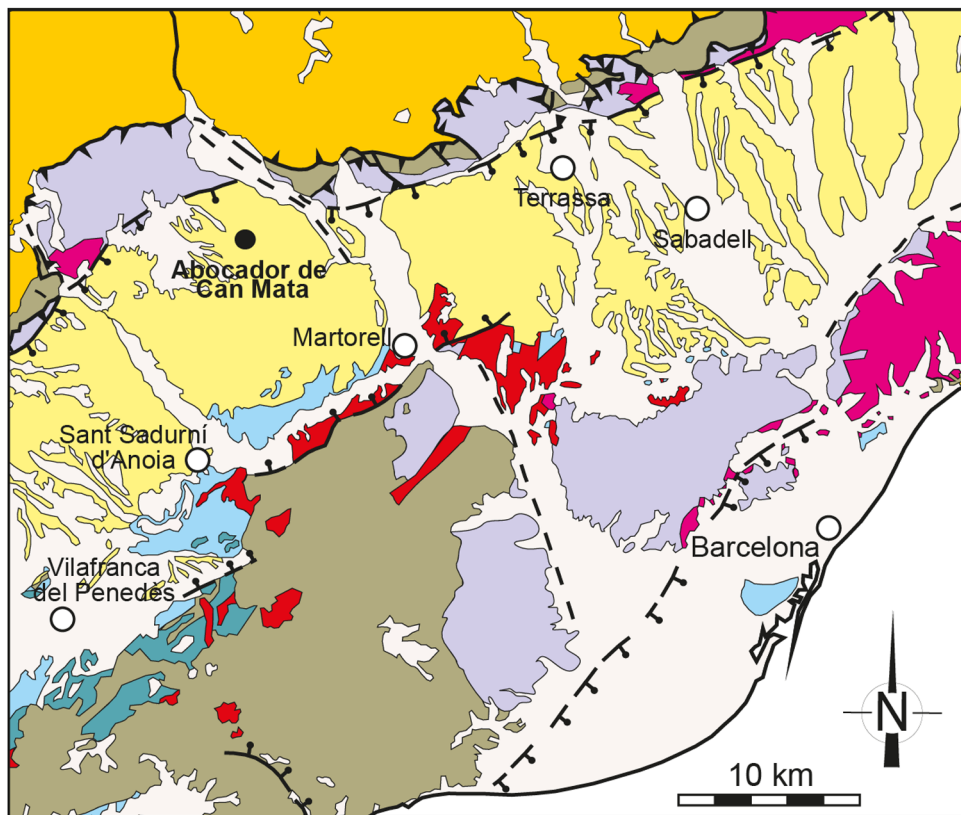
l'Abocador.

Figure 2. *Eomellivora moralesi* sp. nov. from ACM/PTA-A2: a–e, IPS122262 (holotype),

palate in inferior (a), rostral (b), caudal (c), left lateral (d), and right lateral (e) views; f–h,

IPS122212 (paratype), right mandibular fragment with symphysis and premolars, in occlusal

(f), labial (g), and lingual (h) views; i–k, IPS122214 (paratype), right mandibular fragment

with m2, in occlusal (i), labial (j), and lingual (k) views; l–u, complete tooth crowns of the

aforementioned specimens in greater occlusal detail: l, rigth P2; m, left P2; n, right P3; o, left

P3; p, right P4; q, left P4; r, right M1; s, left M1; t, right p2; u, right m2. Images are oriented

with mesial (a, f, I, l–u) or dorsal (b–e, g–h, j–k) on top.

Figure 3. Bivariate plots of buccolingual width (W, in mm) vs. mesiodistal length (L, in mm)

to compare dental size and proportions in *Eomellivora moralesi* sp. nov. with those of other

species of *Eomellivora*. Comparative data were taken from the literature (see Materials and

methods for data sources).

Figure 4. Strict consensus of 3 most parsimonious cladograms of 34 steps. Consistency index = 0.735; retention index = 0.743; rescaled consistency index = 0.546. Bremer and bootstrap (when >50%) support for ingroup clades are depicted above and below nodes, respectively.

Figure 5. Occlusal views of the P3 (a–d), P4 (e–k) and M1 (l–r) of *Eomellivora* species compared (all teeth depicted as from the right side): a, e, l) *Eomellivora moralesi* sp. nov. from ACM/PTA-A2 (IPS122262, holotype; P3 reversed); b, f, m) *Eomellivora piveteaui* from Batallones-3 (Bat-3´13.185; P3 reversed); c, g, n) *Eomellivora ursogulo* from Grebeniki (PIN-No.268, holotype); d, h, o) *Eomellivora wimani* from Shangyingou (PMU-M3692, lectotype); i, p) *E. piveteaui* from Yassiören (MNHN-TRQ-1005, holotype); j, q) *Eomellivora fricki* from Wien XII-Altmannsdorf (NHMW 2016/0065/0001, holotype; reversed); k) *E. fricki* from Can Llobateres 1 (IPS2015); r) *E. fricki* from Los Valles de Fuentidueña (IPS2057). All images are depicted with mesial on top.

a

Terrassa

Sabadell

Abocador de
Can Mata

Martorell

Sant Sadurní
d'Anoia

Barcelona

Vilafranca
del Penedès

EBRO BASIN

VALLÈS-PENEDÈS BASIN

COASTAL RANGES

N

10 km
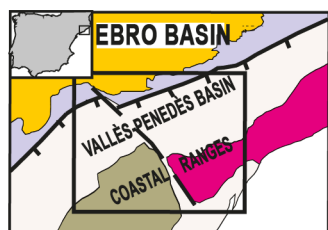
NEOGENE-QUATERNARY

Pliocene and Quaternary sediments

Middle to late Miocene continental units
(Langhian-Tortonian): alluvial fan facies

Miocene marine and transitional units (Late Burdigalian-Langhian):
coralgal carbonate facies

Miocene marine and transitional units (Late Burdigalian-
Serravallian): marls, silts, bioclastic sands and sandstones

Early Miocene continental units (Early and Late Burdigalian):
alluvial fan and shallow lacustrine facies

EBRO FORELAND BASIN INFILL

Paleogene (conglomerates, sandstones, lutites)

PALEOZOIC BASEMENT AND MESOZOIC COVER

Mesozoic (carbonates, sandstones, lutites)

Hercynian intrusive rocks (mostly granitoids)

Paleozoic sedimentary and metamorphic rocks

Fault

Inferred fault

Normal fault

Thrust fault
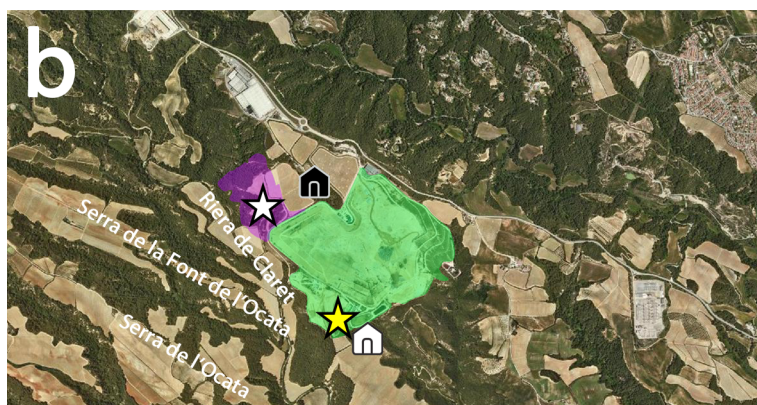
b

Riera de Claret

Serra de la Font de l'Ocata

Serra de l'Ocata

C

PTA-A

Can Mata

1 km

100 m

ACM (2017)   ACM/PTA-A2   Can Mata de la Garriga

ACM (2020)   ACM/BCV1   Can Vila

5 cm

1 cm

Zodiolestes daimonelixensis

Howellictis valentini

Eomellivora moralesi

Eomellivora fricki

Eomellivora piveteaui

Eomellivora hungarica

Eomellivora wimani

Eomellivora ursogulo
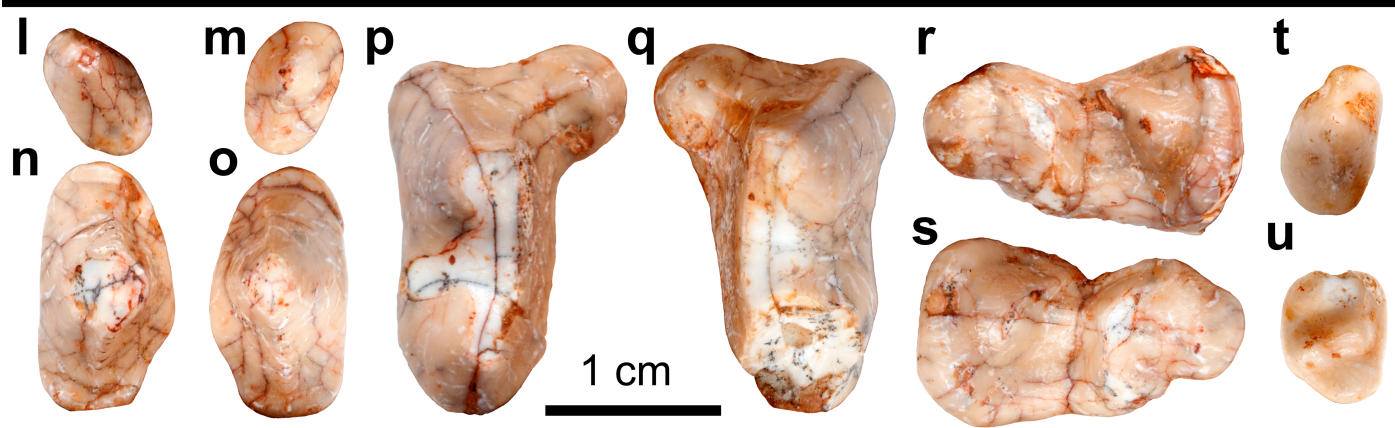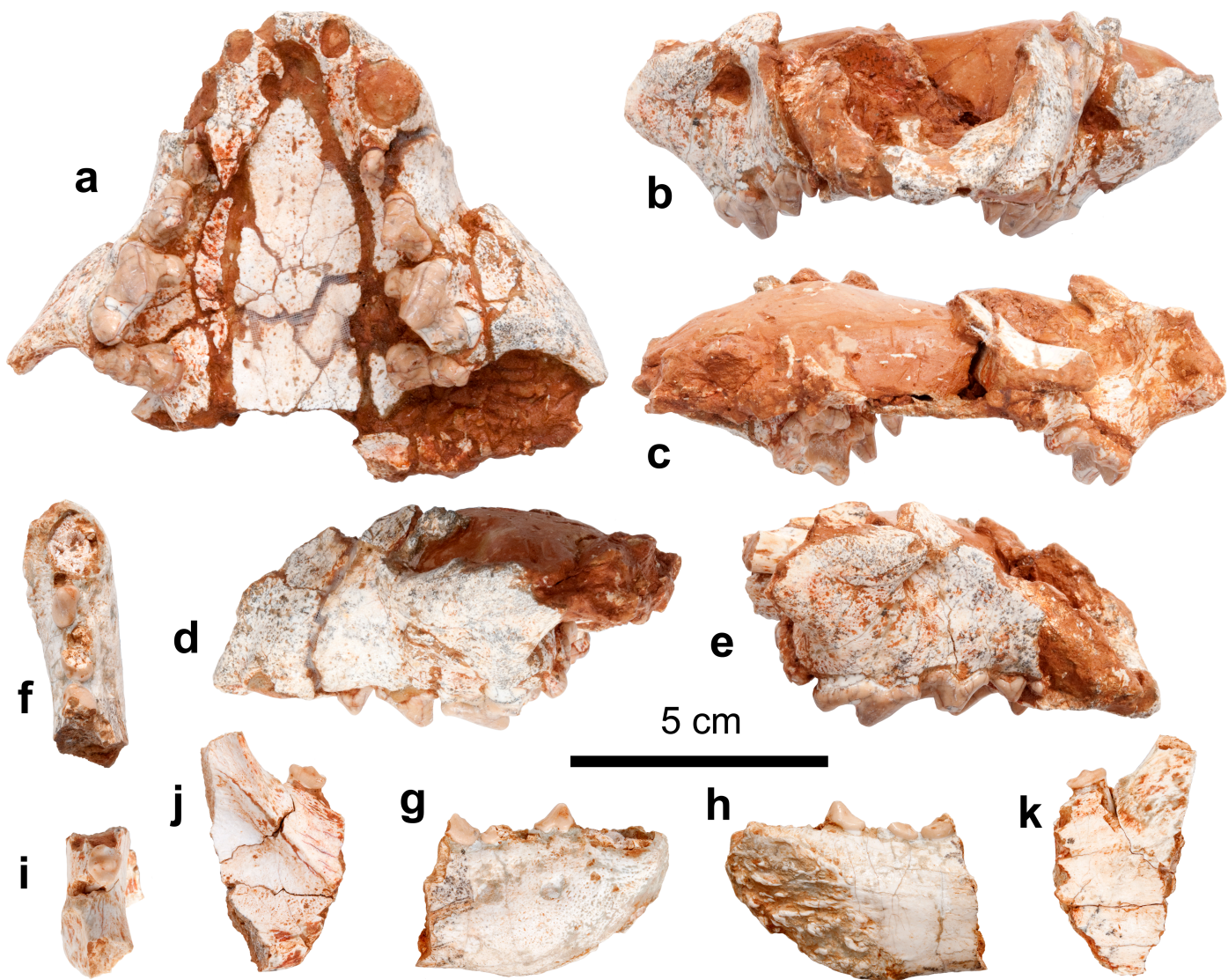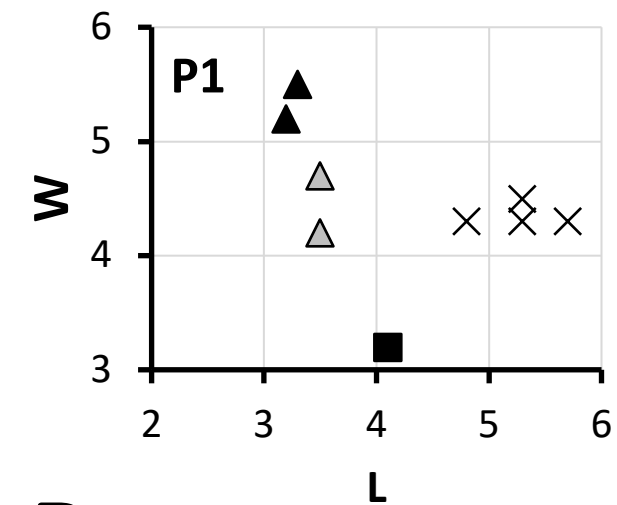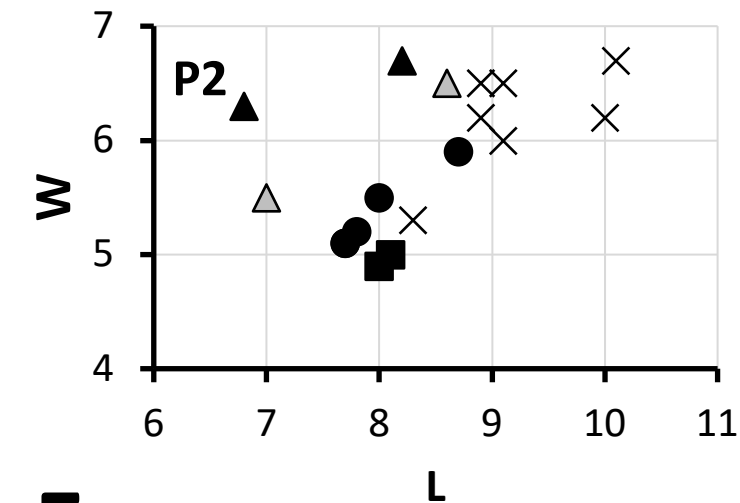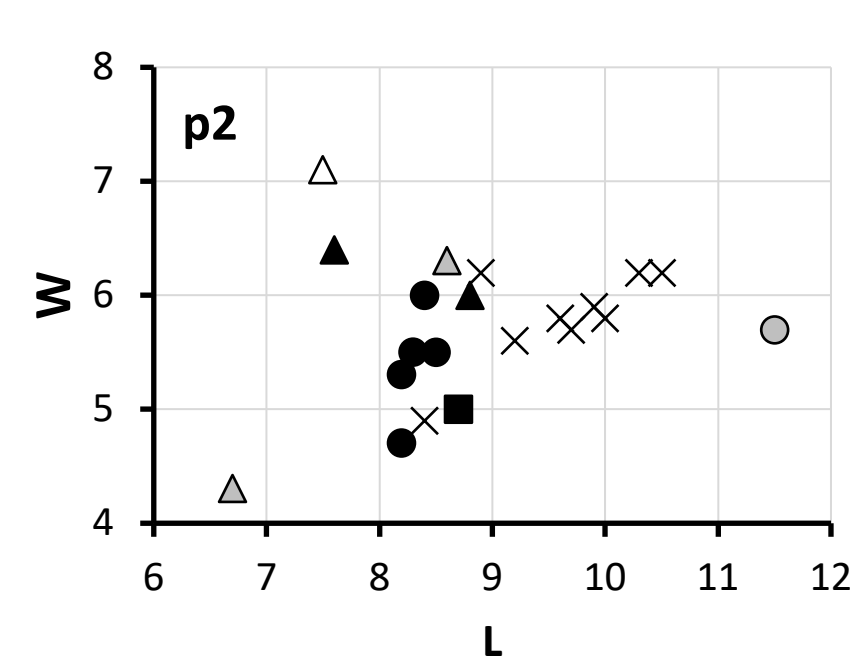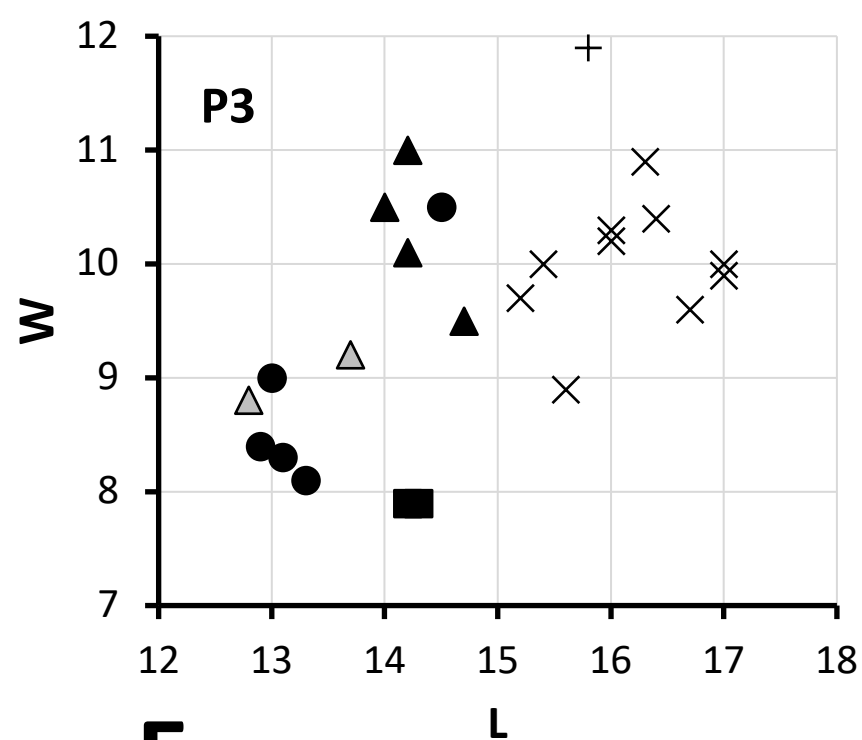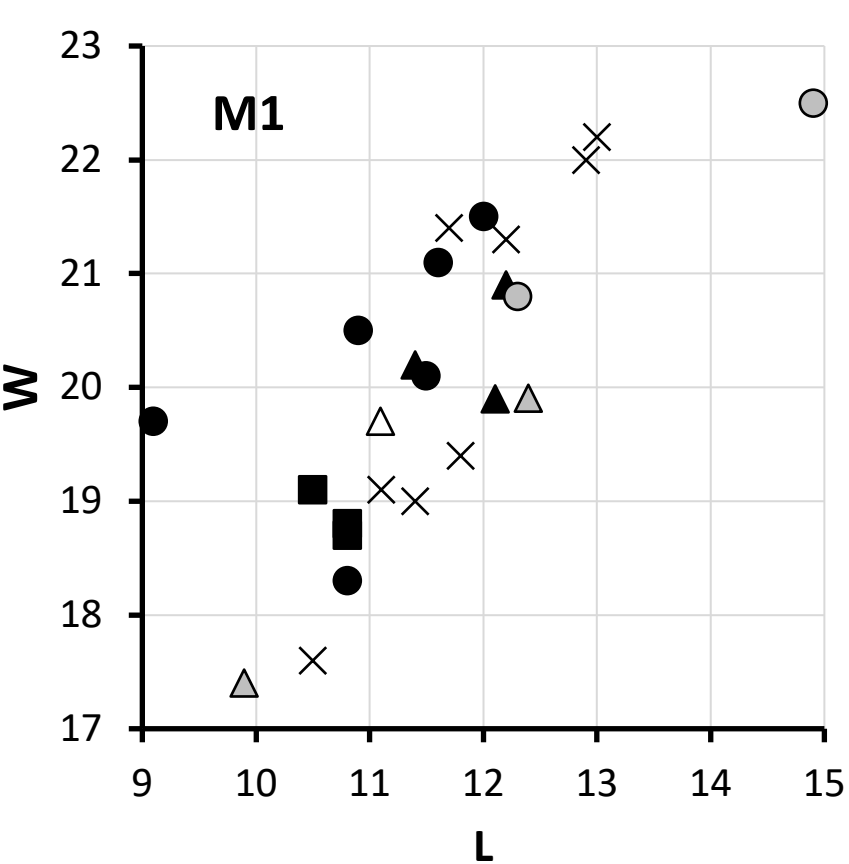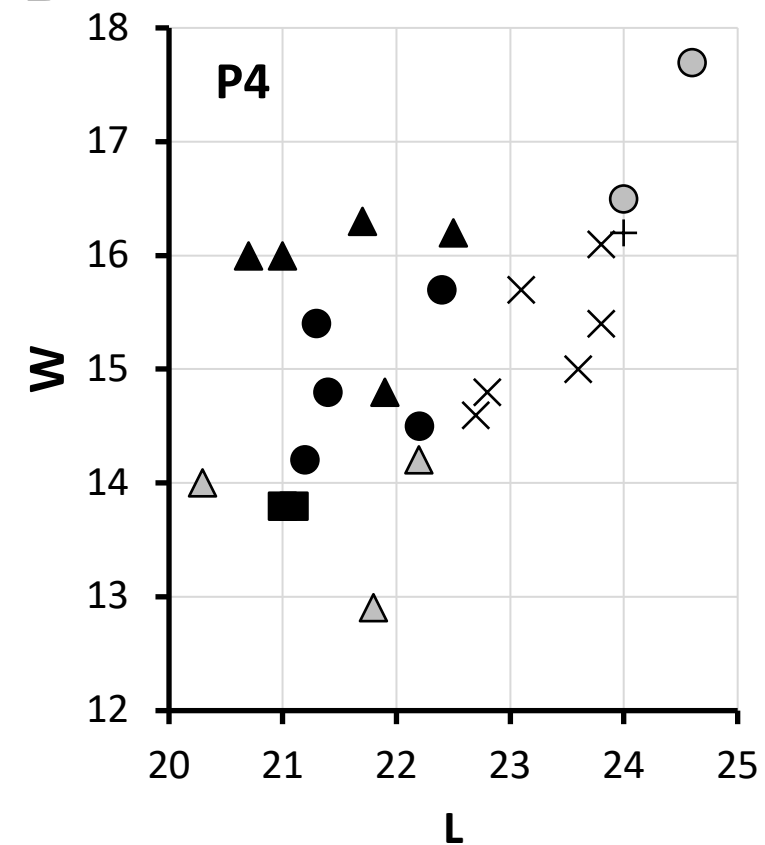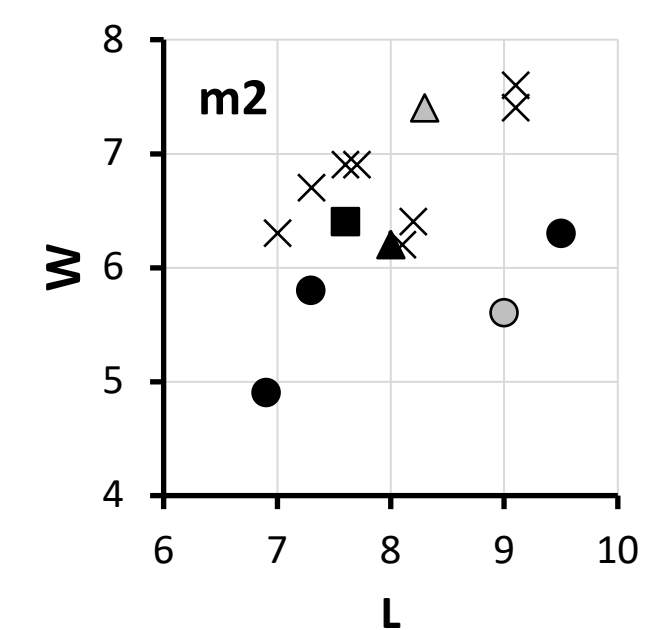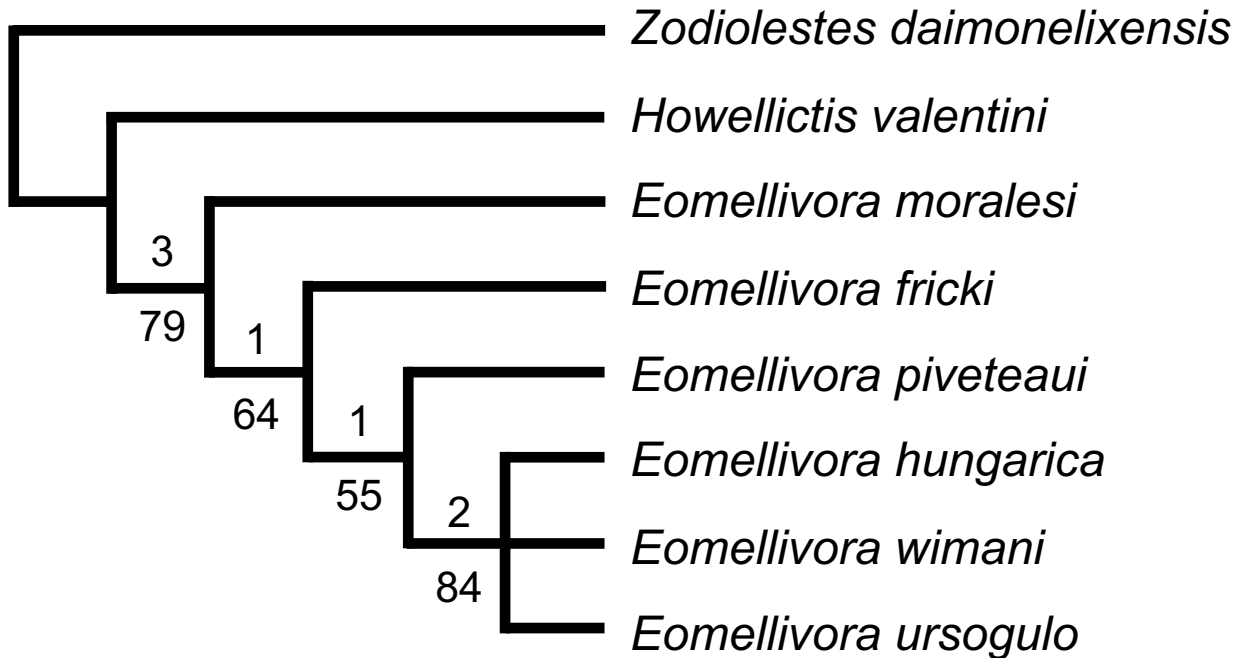
a **b** **c** **d**

Table 1. Character-taxon matrix used in the phylogenetic analysis, following Valenciano & Govender (2020). See also Supplementary Text S1 for

the description of character states. Only parsimony-informative characters for this sample of taxa (bolded) were used in the analysis.

```
                          000000000000000000000000000000000000000000000000000000000000000000000000000000000000000001
          Character #     000000000011111111112222222222333333333344444444445555555555666666666677777777778888888888999999999990
Taxon                     123456789012345678901234567890123456789012345678901234567890123456789012345678901234567890

Eomellivora moralesi      ?110???1??0100000100?10101010011101000100010001?1???1?0?????????????????0?0?????????????????????????
Eomellivora fricki        ??1?11?1???????0???????11?01011110?00120?01?0???????1000101?10?10??11?201?0?????????????????????????
Eomellivora hungarica     ???????1???????????????????111?10110????0???????11001010101111111220101?????????????????????????
Eomellivora piveteaui     11101101??0100010011110101010111101000100010001100011000101010111111111010001010000001111101100002101
Eomellivora wimani        ??10???1010101111011110101010111111111111000100021000211001010101011111111010001?????????????????????
Eomellivora ursogulo      1?1?????1110111110111101010101111111110111001100211002110010101001111111010001?????????????????????
Howellictis valentini     1?0?1101??100100000???11001000120111011001100021000110001010000111011110100110?????????????????11???
Zodiolestes daimonelixensis 110011000100000000000101001100211000010000010010000110000000000011000000000001000110100002000001010
```

Table 2. Dental measurements of *Eomellivora moralesi* sp. nov. from ACM/PTA-A2 based on the holotype (upper teeth) and paratypes (lower teeth). Measurements within parentheses are estimated due to minor damage; those within brackets are estimated based on alveolus size.

Tooth	Left			Right		
	L (mm)	W (mm)	W/L (%)	L (mm)	W (mm)	W/L (%)
I3	[6.0]	[7.4]	[123.3]	—	—	—
C1	[12.8]	[12.0]	[93.8]	—	—	—
P1	—	—	—	4.1	3.2	78.0
P2	8.0	4.9	61.3	8.1	5.0	61.7
P3	14.3	7.9	55.2	14.2	7.9	55.6
P4	(21.0)	13.8	(65.7)	21.1	13.8	65.4
M1	10.8	18.8	174.1	10.8	18.7	173.1
c1	[13.0]	[10.0]	[76.9]	—	—	—
p1	[3.0]	[2.3]	[76.7]	—	—	—
p2	8.7	5.0	57.5	—	—	—
p3	[12.4]	6.4	[51.6]	—	—	—
m2	7.6	6.4	84.2	—	—	—

Table 3. Cranial and mandibular measurements of *Eomellivora moralesi* sp. nov. from

ACM/PTA-A2 based on the holotype (cranium) and paratypes (mandible).

Variable	Measurement (mm)
Length of the preserved cranium	99
Width of the preserved cranium	122
Right infraorbital foramen width	9.8
Right infraorbital foramen height	7.5
Length of I3–C1 diastema	4.5
Mandibular corpus depth below p3	28.7
Mandibular corpus depth below p4	26.3
Mandibular corpus maximum width at c1	18.0
Mandibular corpus maximum width at p3	14.5
Mandibular corpus maximum width at p4	13.5

Supplementary material of "A new species of *Eomellivora* from the latest Aragonian of Abocador de Can Mata (NE Iberian Peninsula)"

David M. Alba[1,*], Josep M. Robles[1], Alberto Valenciano[2], Juan Abella[1,3], Isaac Casanovas-Vilar[1]

[1] Institut Català de Paleontologia Miquel Crusafont, Universitat Autònoma de Barcelona, Edifici ICTA-ICP, c/ Columnes s/n, Campus de la UAB, 08193 Cerdanyola del Vallès, Barcelona, Spain

[2] Departamento de Ciencias de la Tierra and Instituto Universitario de Investigación en Ciencias Ambientales de Aragón (IUCA), Área de Paleontología, Universidad de Zaragoza, C/ Pedro Cerbuna 12, 50009 Zaragoza, Spain

[3] Instituto Nacional de Biodiversidad, Pje. Rumipamba N. 341 y Av. de los Shyris (Parque La Carolina) Quito, Ecuador

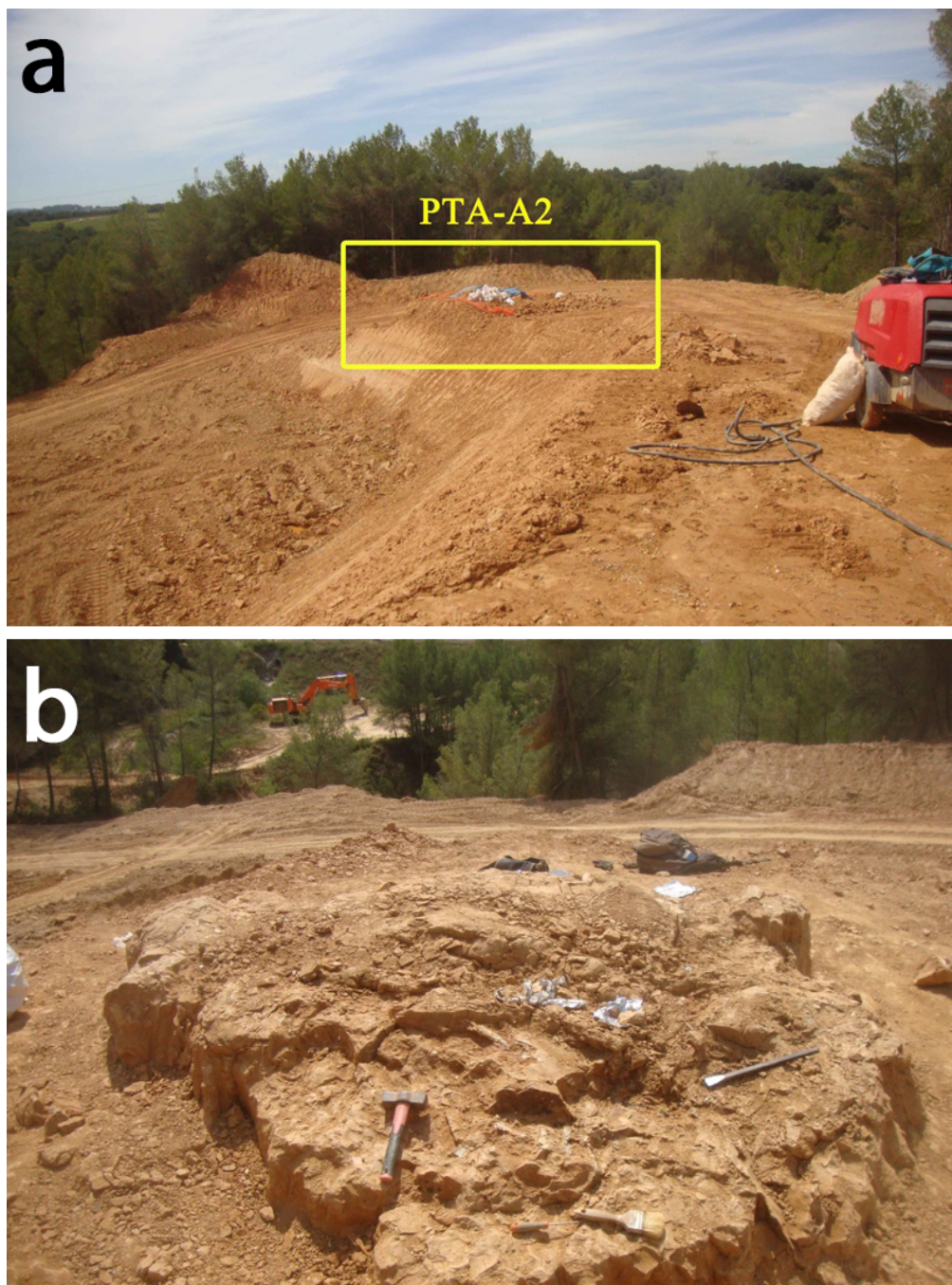*Corresponding author. *E-mail address:* david.alba@icp.cat

Figure S1. General (a) and detailed (b) views of locality ACM/PTA-A2 during excavation in May and June 2019, respectively. © Institut Català de Paleontologia Miquel Crusafont.
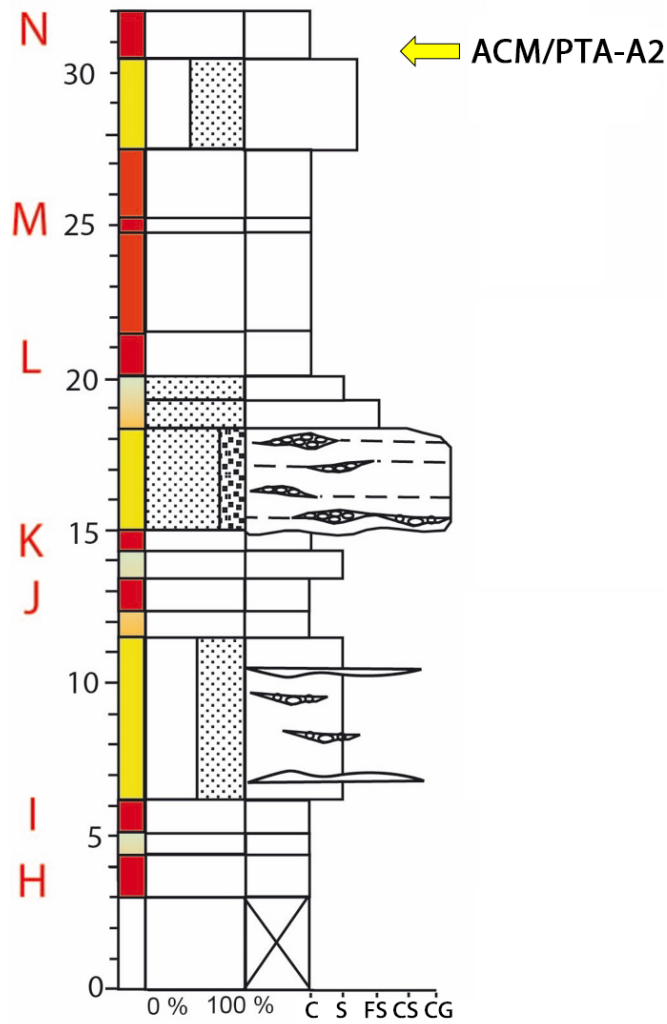
Figure S2. Stratigraphic section of Abocador de Can Mata, sector Préstec de Terres de l'Abocador, subsector A (ACM/PTA-A). Uppercase letters to the left correspond to lithostratigraphic correlation levels, whereas the stratigraphic situation of locality ACM/PTA-A2 (bottom of level N) is indicated with an arrow. Lithology abbreviations: C = claystones; S = siltstones; FS = fine sandstones; CS = coarse sandstones; CG = conglomerates. Note that the previously available composite lithostratigraphic correlation panel for ACM was based on 42 correlation levels (Alba et al. 2017: SOM Fig. S1 and Table S1), of which the uppermost one was level G. The whole stratigraphic section of ACM/PTA-A comprises correlation levels H to N, and is thus located above the ACM composite sequence reported by Alba et al. (2017). The distance between correlation levels G and H is ca. 10 m. Based on currently available data (D.M.A. and J.M.R.'s unpublished data), ACM/PTA-A2 is located in meter 268 of the updated composite sequence, being correlated to C5r.2n with an interpolated age of 11.21 Ma.

Supplementary Text S1. Characters and character states used in the phylogenetic analysis, after Valenciano & Govender (2020).

(1) Posterior lacerate and jugular foramina: "fused" into a single foramen (0); tendency to separate openings with the jugular foramen distolateral to the posterior lacerate foramen (1).

(2) Shape of upper incisor row: parabolic (0); straight (1).

(3) Position of the infraorbital foramen: above P3 (0); above P4 parastyle (1).

(4) Incisive foramen: located at the level of C (0); located at the level of the diastema I3-C (1).

(5) Mastoid process: reduced, located in dorsal view in line with the middle point of the orbit (0); enlarged, located laterally exceeding to the orbit (1).

(6) Relative position of the mastoid and paroccipìtal processes: relatively close (0); mastoid process located mesially to the paroccipital process (1).

(7) Paroccipital process: not reduced (0); reduced (1).

(8) Height of the mandibular corpus: low and thin mandibular corpus (0); high and thick mandibular corpus (1).

(9) Orientation of the I3 cusp: spreader out laterally (0); in line with the cusps of I1-2 (1).

(10) Orientation of Canine: spreader out laterally, with an arrangement of the tip none parallel (0); ventrally directed, with a parallel arrangement of the tip (1).

(11) P1. Present (0); absent (1).

(12) P2. Mesiodistal axis of P2: in line with the tooth row (0); rotated buccolingually (1).

(13) P2. Distal accessory cusp: absent (0); present (1).

(14) P2. Occlusal shape: subrectangular (0); triangular (1).

(15) P2. Buccal wall: rectilinear (0); conspicuous concavity (1).

(16) P3. Robustness ratio [(maximum width/ maximum length) x 100]: slender P3 (less than 60) (0); Robust P3 (60 or more than 60) (1).

(17) P3. Mesial accessory cusp: reduced or absent (0); present (1).

(18) P3. Distal accessory cusp: present (0); absent (1).

(19) P3. Buccal wall: rectilinear wall (0); conspicuous concavity (1).

(20) P3. Basal cingulum: weak (0); strong (1).

(21) P3. Roots: 2 roots (0); 3 roots (1).

(22) P3. Lingual bulge in the middle of the tooth: absent or reduced (0); Well-developed (1).

(23) P4/3 length ratio. Maximum length of P4 in relation to maximum length of P3 ratio [(L P4/L P3) x 100]: less than 170 (0); more than 170 (1).

(24) P4. Robustness ratio [(maximum width/ maximum length) x 100]: slender P4 (less than 60) (0); robust P4 (more than 60) (1).

(25) P4 protocone: low (0); knoblike (1).

(26) P4. Protocone cingulum: weak or absent (0); prominent and complete (1).

(27) P4. Protocone: in front to the mesiobuccal corner (0), mesial to the mesiobuccal corner (1); distally displaced (2).

(28) P4. Parastyle: Absent or weak (0); Strong and low (1); Strong and high (2).

(29) P4. Buccal wall: rectilinear (0); with a pronounced concavity between paracone and metastyle (1).

(30) P4. Basal cingulum surrounding the tooth: weak (0); strong (1).

(31) Relative size between maximum width of M1 and the maximum length of P4: M1 larger than or equal in size to P4 (values >100) (0); M1 smaller than P4 (values between 70-100) (1); M1 much smaller than P4 (values <70) (2).

(32) M1. Robustness ratio [(maximum width on the buccolingual area/ maximum length) x 100]: relatively robust M1 (from 130 to 150) (0); slender M1 (more than 150) (1), very slender M1 (more than 200) (2).

(33) M1. Stylar area: small (0); enlarged (1).

(34) M1. Metacone related to paracone: normal size (0); much reduced (1).

(35) M1. Metaconule: present (0); absent (1).

(36) M1. Protocone position: mesolingually located (0); almost centrally on the middle of the talon (1).

(37) M1. Protocone shape: ridge-shaped (0); conical cusp-like shape (1).

(38) M1. Lingual platform: not completely enclose the protocone (0); completely enclose the protocone (1).

(39) M1. Length of the lingual wall: lesser than the buccal wall (unexpanded lingual platform) (0); longer than the buccal wall (moderately lingual platform) (1); much longer than the buccal wall (much expanded lingual platform) (2).

(40) M1. Lingual platform: oval shape (0); with a concavity in the middle point (1).

(41) M1. Presence of a slender buccolingual crista from the paracone to the protocone: very reduced or absent (0); present (1).

(42) p1. Present (0); absent (1).

(43) p2. Position of the mesiodistal axis of p2: in line with the tooth row (0); buccolingually rotated (1).

(44) p2. Distal accessory cuspid: absent (0); present (1).

(45) p2. Basal cingulum: incomplete and weak (0); complete and strong (1).

(46) p2. Mesial and distal cristids: weak cristids (0); thickened cristids (1).

(47) p2. Robustness ratio [(maximum width/ maximum length) x 100]: slender p2 (less than 50) (0); relatively robust p2 (from 50 to 70) (1); very robust p2 (>70) (2).

(48) p2 length compared to p3: p2 not reduced (0); p2 reduced (1).

(49) p3. Mesial accessory cuspid: absent (0); present (1).

(50) p3. Mesial and distal cristids: weak cristids (0); thickened cristids (1).

(51) p3. Basal cingulum: incomplete and weak (0); complete and strong (1).

(52) p3. Ratio distal thickened of p3 [(maximum width p3/ maximum length p3) x 100]: < 50, p3 elongated (0); from 50-70, p3 with distal expansion (1); > 70 distal part very thick (2).

(53) p4. Length ratio in relation to m1 [(maximum length p4/ maximum length m1) x 100]: from 50 to 60, indicating a relatively not reduced p4 (0); more than 60, indicating a p4 relatively enlarged (1).

(54) p4. Mesial accessory cuspid: absent or poorly developed (0); present, well developed (1).

(55) p4. Distal accessory cuspid: High and well developed (0); low and reduced (1); absent (2).

(56) p4. Mesial and distal cristids: weak cristids (0); thickened cristids (1).

(57) p4. Basal cingulum: incomplete and weak (0); complete and strong (1).

(58) p4. Buccal wall: straight (0); markedly concave (1).

(59) p4. Backward inclination of the main cuspid: practically vertical (90º–80º) (0); with backward inclination (less than 80º) (1).

(60) p4, unworn principal cusp: equals or exceeds height of m1 paraconid (0); lower than m1 paraconid (1).

(61) p4. Distal area: not buccolingually thickened, oval shaped (0); buccolingually thickened, quadrangular shaped (1); rhomboid shaped (2).

(62) p4. Lingual expansion or basal bulge: absent (0); present (1).

(63) m1. Height of protoconid in relation to paraconid: protoconid higher than paraconid (0); protoconid similar in height than the paraconid (1).

(64) m1. Metaconid: Present (0); reduced/absent (1).

(65) m1. Relative length of talonid with respect the total m1 length: the talonid 1/3 of the total length (0); equal or less than 1/4 of the total length (1).

(66) m1. Width talonid ratio [(maximum talonid width/ maximum width in the base of the protoconid-metaconid) x 100]: talonid not reduced (values between 85-100) (0); reduced talonid (< 85) (1).

(67) m1. Height of hypoconid: low (0); high (1).

(68) m1. Position of hypoconid: labially located (0); centrally positioned or almost centrally positioned (1).

(69) m1. Orientation of the hypoconid: almost vertical (0); orientated towards the protoconid (1).

(70) m1. Entoconid: transform in an entocristid (0); absent (1)

(71) m1 talonid: open and shallow basin with a reduced and low entocristid and a beveled lingual wall of the talonid (0); basin lost (1).

(72) m1. Shape of the hypoconid: pyramidal (0); trending to a crest-like shape (1).

(73) m1. Hypoconid size: medium (0); enlarged (1).

(74) m1. Hypoconulid: very reduced to absent (0); present, not reduced (1).

(75) m2. Always present (0); residual presence (present in a low rate <25% of the sample, comprising a reduced alveolus) or absent (1).

(76) m2 paraconid: present (0); (1) very weak or absent (1).

(77) m2. Metaconid: present (0); absent (1).

Postcranial

(78) Humerus. Delto-Pectoral crest most distal part: between the first third and the middle point of the diaphysis (0); exceeding half of the diaphysis (1).

(79) Humerus. Development of the Deltoideus crest: Not very marked, normal development (0); large development, medially enlarged (1).

(80) Humerus. Development of the Pectoral crest: Not very marked, normal development (0); large development, laterally enlarged (1).

(81) Humerus. Supraepicondylar crest: small size (0); enlarged and laterally projected (1).

(82) Humerus. Medial epicondyle: small-sized, not proximodistally enlarged (0); large-sized, proximodistally enlarged and medially projected (1).

(83) Humerus. Distal view of the distal epiphysis: Sub-quadrangular shape (0); rectangular shape, craniocaudally compressed (1).

(84) Ulna. Proximal epiphysis: presence of two tubers (craniomedial and craniolateral one) on the olecranon (0); presence of one or even no tuber on the cranial part of the olecranon (1).

(85) Ulna. Tuber olecrani: Rectilinear, scar for M. triceps brachii proximally projected (0); scar M. triceps brachii medially projected (1).

(86) Ulna. Medial side of the most distal part of the diaphysis: small size and barely visible crest for the M. pronator quadratus, (0); moderate size of the crest for the M. pronator quadratus, occupying the last forth of the diaphysis (1); large development of this crest, medially projected, occupying the last third of the diaphysis (2).

(87) Ulna. Articular circumference: robust, rostrally projected (0); reduced and integrated into the styloid process (1).

(88) Ulna. Index of fossorial ability (IFA) according Rose et al. (2014) x 100: Values lesser than 22, = not fossorial (0); Values equal or higher than 22 = a relatively large olecranon process which is related with semifossorial traits in living badgers (1).

(89) Radius. Proximal view of the proximal epiphysis: Oval- shaped (0); Subrectangular-shaped, craniocaudally reduced (1).

(90) Radius. Radial tuberosity: Robust, oval, with the scar of the insertion of M. brachialis caudally projected (0); rounded scarf with a normal projection (1); barely marked scarf not caudally projected (2).

(91) Radius. Medial side of the most distal part of the diaphysis: rectilinear wall, no visible crest or scarf for the M. pronator quadratus (0); large development of this crest, which occupies the last third of the diaphysis, and is medially projected, comprising a concave surface in the caudal side (1).

(92) Radius. Robustness ratio of the distal epiphysis [(maximum craniocaudal length/ maximum mediolateral length) x 100]: <70, subrectangular shaped (0); > 70 robust distal epiphysis, subquadrangular shape (1).

(93) Radius. Distal epiphysis, medial styloid process: prominent, medially projected and relatively large (0); medium to small size, not medially projected (1).

(94) Radius. Distal epiphysis, carpal articular surface: its medial point is relatively perpendicular to the main axis of the radius (0); its medial point conforms 45 degrees in relation to the main axis of the radius (proximally projected) (1).

(95) Radius. Diaphysis: relatively rectilinear in medial view, non-craniocaudally widened (0); caudally curved at the distal part, comprising a concave surface (1).

(96) Calcaneus. Calcaneal tuber: presence of two processes (medial and lateral) (0); presence of one process or even absence of processes (1).

(97) Calcaneus. Calcaneal robustness index [(width of calcaneal head at widest point including sustentacular facet and the quadratum plantae process/ maximum length of the calnaneus) x 100]: values > 55, calcaneus relatively short (0); values between 55-45 normal length of the calcaneus (1); values < 45 calcaneus relatively elongated (2).

(98) Calcaneus. Calcaneal tuber/calcaneal hell: slender (0); mediolaterally widen (1).

(99) Calcaneus. Sustentacular facet: located close to the body of the calcaneus (0); medially projected (1).

(100) Calcaneus. M. quadratus plantae process laterally expanded (0); M quadratus plantae process reduced and not projected (1).

Table S1. Geographic and temporal distribution of *Eomellivora* species, after Valenciano et al. (2015, 2017, 2019) and this paper.

Species	Age	Locality and country	Taxonomical references	Age references
Eomellivora sp.	11.62 Ma, late Aragonian (MN7+8)	Hammerschmiede 5, Germany	Kirscher et al. (2016)	Kirscher et al. (2016)
Eomellivora moralesi sp. nov.	11.21 Ma, late Aragonian (MN7+8)	ACM/PTA-A2, Spain	This paper	This paper
Eomellivora fricki	Earliest Pannonian C, early Vallesian (MN9)	Gaiselberg, Austria	Zapfe (1948); Valenciano et al. (2017)	Valenciano et al. (2017)
Eomellivora fricki	Pannonian D, early Vallesian (MN9)	Wien XII-Altmannsdorf, Austria	Pia (1939); Valenciano et al. (2017)	Valenciano et al. (2017)
Eomellivora fricki	9.76 Ma, early Vallesian (MN9)	Can Llobateres 1, Spain	Petter (1963); Crusafont-Pairó (1972); Valenciano et al. (2019)	Casanovas-Vilar et al. (2016)
Eomellivora fricki	Early Vallesian (MN9)	Los Valles de Fuentidueña, Spain	Crusafont-Pairó & Ginsburg (1973); Ginsburg et al. (1981); this study	Alberdi et al. (1981)
Eomellivora piveteaui	Vallesian (MN9–MN10)	Yassiören, Turkey	Ozansoy (1965); Wolsan & Semenov (1996); Valenciano et al. (2015)	Kappelman et al. (2003)
Eomellivora piveteaui	Vallesian (MN9–MN10)?	Wissberg, Germany	Tobien (1955); Morlo (1997)	Böhme et al. (2012); Pickford & Pourabrisham (2013)
Eomellivora piveteaui	Late Vallesian (MN10)	Kalfa (=Calfa), Moldova	Lungu (1978); Wolsan & Semenov (1996)	Nesin and Nadachowsky (2001)
Eomellivora piveteaui	Late Vallesian (MN10)	Buzhor 1 (= Bujor 1), Moldova	Pevner et al. (2013)	Nesin and Nadachowsky (2001)
Eomellivora piveteaui	9.43–9.31 Ma, late Vallesian (MN10)	Ravin de la Pluie, Greece	Koufos (2012)	Sen et al. (2000)
Eomellivora piveteaui	Subzone J2 (~9.6–9.3 Ma), late Vallesian (MN10)	Batallones-3, Spain	Valenciano et al. (2015)	Peláez-Campomanes et al. (2017)
Eomellivora piveteaui	Subzone J2 (~9.6–9.3 Ma), late Vallesian (MN10)	Batallones-10, Spain	Valenciano et al. (2015)	Peláez-Campomanes et al. (2017)
Eomellivora sp.	Early Turolian (MN11)	Dorn-Dürkheim 1, Germany	Morlo (1997)	Franzen et al. (2013)
Eomellivora wimani	9.79–9.76 Ma, Bahean	Shangyingou (Sang-Yin-Kou, Lantian Basin locality 12), China	Zdansky (1924); Wolsan & Semenov (1996)	Kaakinen (2005); Zhang et al. (2013)

Eomellivora wimani	8.95 Ma, Bahean	Liuwangou (Liu-Wan-Kou, Lantian Basin locality 31), China	Zdansky (1924); Wolsan & Semenov (1996)	Kaakinen (2005); Zhang et al. (2013)
Eomellivora wimani	Turolian (MN12?)	Győrszentmárton 2 (=Pannonhalma), Hungary	Kretzoi (1965); Wolsan & Semenov (1996)	Gasparik (2001)
Eomellivora wimani	~7.2–7.1 Ma, middle Turolian (MN12)	Chimishliya (=Cimișlia), Moldova	Simionescu (1938); Wolsan & Semenov (1996)	Vangengeim and Tesakov (2008), reinterpreted; Vasiliev et al. (2011)
Eomellivora wimani	~7.5–7.2 Ma, middle Turolian (MN12)	Novaya Emetovka 2, Ukraine	Orlov (1948); Wolsan & Semenov (1996)	Vangengeim and Tesakov (2008), reinterpreted; Vasiliev et al. (2011)
Eomellivora wimani	Early Hemphillian (Hh2)	Kern River Formation site 50, USA	Stock & Hall (1933); Wolsan & Semenov (1996)	Woodburne (2004); Janis et al. (2008)
Eomellivora wimani	Late Clarendonian (Cl3)	North Tejon Hills Local Fauna, USA	Baskin (1988)	Woodburne (2004); Janis et al. (2008)
Eomellivora wimani	8.2-7.1 Ma, Bahean	Yuanmou-Xiahoe, China	Zong (1994)	Zhu et al. (2005); Dong & Qi (2013)
Eomellivora cf. *wimani*	7.14-6.25 Ma, Baodean	Lufeng hominoid locality, Shihuiba, China	Qi (1985)	Qi et al. (2006); Dong & Qi (2013)
Eomellivora sp.	Early Hemphillian (Hh1)	Higgins Local Fauna (= Sebits Ranch)	Dalquest and Patrick (1989)	Janis et al. (2008)
Eomellivora sp.	Early Hemphillian (Hh1)	Dove Spring Local Fauna	Baskin (1988)	Janis et al. (2008)
Eomellivora sp.	Early Hemphillian (Hh1)	Smiths Valley Local Fauna	Baskin (1988)	Janis et al. (2008)
Eomellivora ursugulo	Early–middle Turolian (MN11–MN12)	Grebeniki, Ukraine	Orlov (1948); Wolsan & Semenov (1996)	Vislobokova et al. (2001), Vangengeim and Tesakov (2008), reinterpreted; Vasiliev et al. (2011)
Eomellivora ursugulo	Middle–late Turolian (MN12–MN13)	Taralik–Cher, Russia	Lavrov & Gimranov (2018)	Lavrov & Gimranov (2018)
Eomellivora hungarica	Late Turolian (MN13)	Polgárdi 2, Hungary	Kretzoi (1942); Wolsan & Semenov (1996)	Freudenthal and Kordos (1989)
Eomellivora sp.	11.15–11.06 Ma, early Vallesian (MN9)	Gritsev (=Grytsiv), Ukraine	Wolsan & Semenov (1996)	Korotkevich et al. (1985); Kirscher et al. (2016)

| *Eomellivora* sp. | Early Vallesian (MN9) | Borský Svätý Jur, Slovakia | Lupták (1995) | Sabol et al. (2004) |
| *Eomellivora* sp. | Early Turolian (MN11) | Csákvár, Hungary | Kretzoi (1942); Wolsan & Semenov (1996) | Mein (1999) |

Supplementary references

Alberdi MT, López N, Morales J, Sesé C, Soria D. 1981. Bioestratigrafía y biogeografía de la fauna de mamíferos de los Valles de Fuentidueña (Segovia). Estud Geol. 37:503–511.

Baskin JA. 1998. Mustelidae. In: Janis CM, Scott KM, Jacobs LL, editors. Evolution of Tertiary mammals of North America. Volume 1: Terrestrial carnivores, ungulates, and ungulatelike mammals. Cambridge: Cambridge University Press; p. 152–173.

Böhme M, Aiglstorfer M, Uhl D, Kullmer O. 2012. The antiquity of the Rhine River: stratigraphic coverage of the Dinotheriensande (Eppelsheim Fomation) of the Mainz Basin (Germany). PLoS ONE. 7:e36817.

Casanovas-Vilar I, Garcés M, Van Dam J, García-Paredes I, Robles JM, Alba DM. 2016. An updated biostratigraphy for the late Aragonian and Vallesian of the Vallès-Penedès Basin (Catalonia). Geol Acta. 14:195–217.

Crusafont-Pairó, M. 1972. Les *Ischyrictis* de la transition Vindobonien-Vallésien. Palaeovertebrata. 5:253–260.

Crusafont-Pairó M, Ginsburg L. 1973. Les carnassiers fossiles de Los Vallès de Fuentiduena (Ségovie, Espagne). Bull Mus Natl Hist Nat. 131:29–45.

Dalquest WW, Patrick DB. 1989. Small mammals from the early and medial Hemiphillian of Texas, with descriptions of a new bat and a gopher. J Vertebr Paleontol. 9:78–88.

Dong W, Qi G-Q. 2013. Hominoid-producing localities and biostratigraphy in Yunnan. In: Wang X, Flynn LJ, Fortelius M, editors. Fossil mammals of Asia: Neogene biostratigraphy and chronology. New York: Columbia University Press, p. 1–25.

Franzen JL, Pickford M, Costeur L. 2013. Palaeobiodiversity, palaeoecology, palaeobiogeography and biochronology of Dorn-Dürkheim 1—a summary. Palaeobiodiv Palaeoenviron. 93:277–284.

Freudenthal M, Kordos L. 1989. *Cricetus polgardensis* sp. nov. and *Cricetus kormosi* Schaub, 1930 from the Late Miocene Polgárdi localities (Hungary). Scripta Geol. 89:71–100.

Gasparik M. 2001. Neogene proboscidean remains from Hungary; an overview. Frag Palaeontol Hung. 19:61–77.

Ginsburg L, Morales J, Soria D. 1981. Nuevos datos sobre los carnívoros de los Valles de Fuentidueña (Segovia). Estud Geol. 37:383–415.

Koufos GD. 2012. New material of Carnivora (Mammalia) from the Late Miocene of Axios Valley, Macedonia, Greece. C R Palevol. 11:49–64.

Janis CM, Gunnell GF, Uhen MD, editors. 2008. Evolution of Tertiary Mammals of North America: Volume 2, Small Mammals, Xenarthrans, and Marine Mammals. Cambridge: Cambridge University Press.

Kaakinen A. 2005. A long terrestrial sequence in Lantian - a window into the late Neogene palaeoenvironments of northern China [PhD dissertation]. Helsinki: University of Helsinki.

Kappelman J, Duncan A, Feseha M, Lunkka J-P, Ekart D, Ryan TM, Swisher CC III. 2003. Chronology. In: Fortelius M, Kappelman J, Sen S, Bernor RL, editors. Geology and paleontology of the Miocene Sinap Formation, Turkey. New York: Columbia University Press; p. 41–66.

Kirscher U, Prieto J, Bachtadse V, Aziz HA, Doppler G, Hagmaier M, Böhme M. 2016. A biochronologic tie-point for the base of the Tortonian stage in European terrestrial settings: Magnetostratigraphy of the topmost Upper Freshwater Molasse sediments of the North Alpine Foreland Basin in Bavaria (Germany). Newslett Stratigr. 49:445–467.

Korotkevich E, Kushniruk V, Semenov Y, Chepaliga A. 1985. A new middle Sarmatian vertebrate fauna locality in Ukraine. Vestnik Zoologii. 29:81–82 (in Russian).

Kretzoi M. 1942. *Eomellivora* von Polgárdi und Csákvár. Föld Közl. 72:318–323.

Kretzoi M. 1965. Die Hipparion-Fauna von Győrszentmárton in NW-Ungarn. Ann hist-nat hungar. 57:127–143.

Lavrov AV, Gimranov DO. 2018. First finding of a representative of giant mustelids of the genus *Eomellivora* (Carnivora, Mustelidae) in Russia (Tuva, Upper Miocene). Doklady Biol Sci. 480:82–84.

Lungu AN. 1978. Hipparion Fauna of Middle Sarmatian of Moldova: Carnivores. Kishinev: Shtintsa (in Russian).

Lupták P. 1995. First evidence of the Turolian carnivorous species *Perunium ursogulo* Orlov, 1948 (*Mustelidae, Mammalia*) from Slovakia. Slovak Geol Magaz. 2:171–174.

Mein P. 1999. European Miocene mammal biochronology. In: Rössner GE, Heissig K, editors. The Miocene land mammals of Europe. Munich: Verlag Dr. Friedrich Pfiel; p. 25–38.

Morlo M. 1997. Die Raubtiere (Mammalia, Carnivora) aus dem Turolium von Dorn-Dürkheim 1 (Rheinhessen). Teil 1: Mustelida [sic], Hyaenidae, Percrocutidae, Felidae. Cour Forsch-Inst Senck. 197:11–47.

Nesin VA, Nadachowsky A. 2001. Late Miocene and Pliocene small mammal faunas (Insectivora, Lagomorpha, Rodentia) of southeastern Europe. Acta Zool Cracov. 44:107–135.

Orlov YU. 1948. *Perunium ursogulo* Orlov, a new gigantic extinct mustelid (a contribution to the morphology of the skull and brain and to the phylogeny of Mustelidae). Acta Zool. 29:63–105.

Ozansoy F. 1965. Étude des gisements continentaux et des mammifères du Cénozoïque de Turquie. Mém Soc Géol Fr. 44:1–92.

Qi G. 1985. A preliminary report on Carnivora from the *Ramapithecus* locality, Lufeng, Yunnan. Acta Anthropol Sin. 4:33–43.

Peláez-Campomanes P, Morales J, Álvarez Sierra MA, Hernández V. 2017. La edad de los yacimientos del Cerro de los Batallones. In: La colina de los tigres dientes de sable. Los yacimientos miocenos del Cerro de los Batallones (Torrejón de Velasco, Comunidad de Madrid). Madrid: Comunidad de Madrid; p. 147–161.

Petter G. 1963. Contribution a l'étude des Mustélidés des bassins néogènes du Vallès-Pénédès et de Calatayud-Teruel. Mem Soc Géol Fr. 97:5–44.

Pevner MA, Lungu AN, Vangengeym EA, Basilyan AE. 2013. Occurrences of Vallesian-age *Hipparion* fauna in Moldavia and their placement on the magnetic polarity scale. Int Geol Rev. 29:140–150.

Pia J. 1939. Ein riesiger Honingsdachs (Mellivorine) aus dem Unterpliozän von Wien. Ann Naturhist Mus Wien. 50:537–583.

Pickford M, Purabrishami Z. 2013. Deciphering Deinotheriensande deinotheriid diversity. Palaeobiodiv Palaeoenv. 93:121–150.

Qi G,Dong W, Zheng L, Zhao L, Gao F, Yue L, Zhang Y. 2006. Taxonomy, age and environment status of the Yuanmou hominoids. Chin Sci Bull 51:704–712.

Sabol M, Joniak P, Holec P. 2004. Succession(-s) of mammalian assemblages during the Neogene – A case study from the Slovak part of the Western Carpathians. Scripta Fac Sci Nat Univ Masaryk Brunensis. 31–32:65–84.

Sen S, Koufos GD, Kondopoulou D, de Bonis L. 2000. Magnetostratigraphy of the late Miocene continental deposits of the lower Axios valley, Macedonia, Greece. Geol Soc Greece Spec Publ. 9:197–206.

Simionescu I. 1938. Mamiferele pliocene de la Cimişlia (România). I Carnivore. Academia Română. Publicaţiunile fondului Vasile Adamachi. 9(50):1–30.

Stock C, Hall ER. 1933. The Asiatic genus *Eomellivora* in the Pliocene of California. J Mammal. 14:63–65.

Tobien H. 1955. Neue und wenig bekannte Carnivoren aus den unterpliozänen Dinotheriensanden Rheinhessens. Notizbl Hess Landesamt Bodenforsch Wiesbaden. 83:7–31.

Valenciano A, Abella J, Sanisidro O, Harstone-Rose A, Álvarez-Sierra MÁ, Morales J. 2015. Complete description of the skull and mandible of the giant mustelid *Eomellivora piveteaui* Ozansoy, 1965 (Mammalia, Carnivora, Mustelidae) from Batallones (MN10), Late Miocene (Madrid, Spain). J Vertebr Paleontol. 35:e934570.

Valenciano A, Abella J, Göhlich UB, Ángeles Álvarez-Sierra M, Morales J. 2017. Re-evaluation of the very large *Eomellivora fricki* (Pia, 1939) (Carnivora, Mustelidae, Mellivorinae) from the late miocene of Austria. Palaeontol Electron. 20:17A.

Valenciano A, Jiangzuo Q, Wang S, Li C, Zhang X, Ye J. 2019. First record of *Hoplictis* (Carnivora, Mustelidae) in East Asia from the Miocene of the Ulungur River Area, Xianjiang, Northwest China. Acta Geol Sin. 93:251–264.

Valenciano A, Govender R. 2020. New fossils of *Mellivora benfieldi* (Mammalia, Carnivora, Mustelidae) from Langebaanweg, 'E' Quarry (South Africa, Early Pliocene): Re-evaluation of the African Neogene mellivorines. J Vertebr Paleontol. 40:e1817754.

Vangengeim EA, Tesakov A. 2008. Maeotian mammalian localities of Eastern Paratethys: magnetochronology and positon in European continental scales. Stratigr Geol Correlation. 16:437–450.

Vasiliev I, Iosifidi AG, Khramov AN, Krijgsman W, Kuiper K, Langereis CG, Popov VV, Stoica M, Tomsha VA, Yudin SV. 2011. Magnetostratigraphy and radio-isotope dating of upper Miocene–lower Pliocene sedimentary successions of the Black Sea Basin (Taman Peninsula, Russia). Palaeogeogr Palaeoclimatol Palaeoecol. 310:163–175.Vislobokova I, Sotnikova M, Dodonov A. 2001. Late Miocene - Pliocene mammalian faunas of Russia and neighbouring contries. Boll Soc Paleontol Ital. 40:307–313.

Woodburne MO, editor. 2004. Late Cretaceous and Cenozoic Mammals of North America: Biostratigraphy and Geochronology. New York: Columbia University Press.

Woslan M, Semenov YA. 1996. A revision of the late Miocene mustelid carnivoran *Eomellivora*. Acta Zool Cracov. 39:593–604.

Zapfe H. 1948. Neue Funde von Raubtieren aus dem Unterpliozän des Wiener Beckens. Sitz-Ber Öst Akad Wiss math-naturwiss Kl. 157:243–262.

Zdansky O. 1924. Jungtertiäre carnivoren Chinas. Palaeontol Sin C. 2:1–149.

Zhang Z-Q, Kaakinen A, Liu L-P, Lunkka JP, Sen S, Gose WA, Qiu Z-D, Zheng S-H, Fortelius M. 2013. Mammalian biochronology of the late Miocene Bahe Formation. In: Zhang X, Flynn LJ,

Fortelius M, editors. Fossil Mammals of Asia: Neogene Biostratigraphy and Chronology. New York, N.Y: Columbia University Press; p. 187–202.

Zhu R, Liu Q, Yao H, Guo Z, Deng C, Pan Y, Lü L, Chang Z, Gao F. 2005. Magnetostratigraphic dating of hominoid-bearing sediments at Zhupeng, Yuanmou Basin, southwestern China. Earth Planet Sci Lett 236:559–586.

Zong G. 1994. On stratigraphic subdivision of hominoid fossil localities of Yuanmou, Yunnan. Hum Evol. 9:209–213.